Rock-property–structural-geology synergy at work in Broken Hill

A case for structural control of linear magnetic anomalies

John W. Giddings[1], George M. Gibson[1], & David W. Maidment[1]

The delivery of a new generation of high-resolution aeromagnetic data for the Broken Hill Block (BHB; Haren et al. 1997: Exploration Geophysics, 28, 235–241) has played a significant role in helping the Broken Hill Exploration Initiative (BHEI) successfully achieve its brief of stimulating exploration activity (Denham et al. 1998: AGSO Record 1998/25, 13–16) in the region. Underpinning geological realism in interpretations of those data, however, is our understanding of what we are tracing with the aeromagnetic anomalies: the more informed our understanding is, the more likely the interpretations will increase the chance of success in exploration. We present here a brief look at a combined rock-property–structural-geology study which clearly demonstrates that linear magnetic anomalies in the BHB can be structurally controlled. This outcome thus challenges the long-held view that such anomalies reflect stratigraphy, and introduces a cautionary note into their use as markers for extrapolating lithology under cover (Maidment et al. this issue, pp. 5–7).

The linear magnetic anomalies we chose to study are part of a broad belt that sweeps across the BHB from north to southwest, and changes strike in the process from north-northeasterly to northeasterly (Fig. 4). Our more informed understanding of those anomalies and our assessment of the significance of the different parameters employed in magnetic modelling is based on combined magnetic field profiling, magnetic minerals determination, measurements of magnetic remanence and anisotropy of magnetic susceptibility, and detailed geological and structural mapping along traverses orthogonal to the strike of the anomalies. We targeted three anomalies, located from north to south (Fig. 4):

- north of Waukaroo Bore (WB) — trending ~27°E and hosted by the Sundown Group;
- northwest of Acacia Vale homestead (AV) — trending ~38°E and hosted by the Thackaringa Group; and
- the Sculptures/Archery Range area (SA), northwest of Broken Hill — trending ~45°E and hosted by the Sundown Group.

Apart from the Sculptures anomaly (for which the traversing and total field measurements were conducted by the New South Wales Department of Mineral Resources, a BHEI collaborator), our traverses were ~500 m long to ensure complete capture of anomaly profiles. Total magnetic field measurements were recorded every 5 m. Susceptibility measurements were made every 10 m, and helped locate the boundaries of the anomalous zones.

Oriented cores of rock were collected along traverses for magnetic property measurements.

Magnetic properties and modelling

Using AGSO's sensitive Czech-built KLY3 Kappabridge (Giddings & Klootwijk 1997: AGSO Research Newsletter 26, 7–9), we identified the magnetic mineral systems in the anomalous zones from the temperature (T) variation of magnetic susceptibility (k) between –195°C and 700°C. Without exception, strongly magnetic samples yield k/T curves that indicate pure end-member magnetite in the titanomagnetite solid-solution series $Fe_{3-x}Ti_xO_4$ (x=0, magnetite), confirming geological evidence for magnetite as the source of these anomalies. Importantly, for the susceptibility anisotropy work, there is no indication of pyrrhotite (Fe_7S_8), an important magnetic mineral after the iron oxides but one that has a strong anisotropy related to its crystal structure.

In keeping with the ideas that certain BHB structural fabrics are magnetite-enriched, we looked at whether a relationship exists between the magnetite and petrofabric by measuring the anisotropy of magnetic susceptibility (AMS) on the KLY3 (Giddings & Klootwijk 1997: op. cit.). This technique detects the presence of any preferred plane (fabric) of maximum susceptibility (the k_{max}–k_{int} axial plane, whose pole is the k_{min} axis), and for magnetite is primarily grain-shape dominated (Borradaile & Henry 1997: Earth Science Reviews, 42, 49–93). The AMS results (Fig. 6) demonstrate that indeed a well-defined, steeply dipping magnetic fabric is present for each anomaly, and that its orientation varies between anomalies. A simple pattern emerges: southwards from WB through AV to SA, the magnetic fabric plane veers from an azimuth of 19°E and steep dip of 82° ESE (WB, anomaly trend ~27°E), through 38°E and dip of 74°SE (AV, anomaly trend ~38°E), to 46°E and dip of 77°SE (SA, anomaly trend ~45°E). This pattern mirrors that of the structurally mapped S_3 fabric of Gibson (1999: Minfo, Department of Mineral Resources, NSW, 62, 10–12; Fig. 5), both in azimuth and dip (compare stereograms, Figs. 6 and 5). Importantly, the anomaly trends lie along the magnetic fabric trends and hence S_3.

We investigated source body geometry by modelling the magnetic profiles in detail; our rock-property parameters provided a guide to the geological integrity of this work. The profiles, interpretations, and geological cross-sections are illustrated for the WB (Fig. 7) and AV (Fig. 8) anomalies. The shapes of the

magnetic profiles indicate that each is a composite of two sources: a buried (20–50 m below the surface), steeply dipping (~80°ESE — WB; ~70°SE —AV) tabular body (~125 m wide and of great depth extent) that gives the gross shape of the profile; and a number of narrower near-surface bodies that extend down to the deeper body and give high-frequency detail to the profile. These thin tabular bodies mimic the observed and marked spatial variation in surface susceptibility (up to two orders of magnitude within metres) that reflects the inhomogeneous distribution of magnetite within the anomalous zones.

Modelling with induced magnetisation alone and in conjunction with magnetic remanence enabled us to assess the importance of remanence to modelling. The initial remanence directions (freed of temporary components acquired before measurement and of lightning-struck samples) of both anomalies are moderately steep upward-pointing (normal, in the vicinity of the Earth's field) and downward-pointing (reverse), and obliquely streaked in between. We find that the reinforcement of the induced magnetisation by the normal remanence is markedly diminished in its importance by the counteracting reverse and oblique remanence, to the extent that the mean remanent field magnetisations are 4–8 times smaller than individual sample magnetisations. As a result, we find that, for these magnetite-sourced linear anomalies, remanence may be ignored in modelling the deeper tabular features, but that individual sample remanences are useful for getting the best fit to the high-frequency detail caused by the near-surface features. In fact, the difference between models (induced only and induced plus remanence) is essentially one of repositioning the less important near-surface bodies to realign the computed profile for the effect of remanence: the shape and dip of the main tabular bodies remain unchanged.

Structural control of anomalies by S_3

How do the models fit with the mapping and AMS data? We note that the dip and dip sense required of the tabular bodies by the shape of the anomaly profiles (Figs. 7, 8) are consistent with the dip and dip sense of the magnetic fabrics measured for the anomalous zones (Fig. 6) and that those fabrics are the S_3 fabric (Fig. 5). Hence the tabular bodies must represent the magnetite-rich S_3 fabric.

For WB, the geological cross-sections (Fig. 7) show that the enveloping surface to S_0 (bedding) dips gently to the NE and SW. However, we demonstrated that the anomalous zone here dips ~80°ESE and is the magnetite-rich S_3 fabric. Clearly, this is a case of

an anomaly controlled by structure, not stratigraphy: magnetite-impregnation of S_3 was probably associated with circulating fluids. Results (not illustrated) indicate a similar origin for the SA anomaly. For AV (Fig. 8), the interpretation is equivocal: S_0 and S_3 have similar steep dips so the case for structural control can be challenged on the basis that S_3 could have inherited a pre-existing magnetite-rich S_0 fabric (bedding — stratigraphic control).

Irrespective of the control mechanism for the AV anomaly, we have added another cautionary note to others concerning the use of linear anomalies for mapping geology in concealed areas: although some undoubtedly reflect lithology, others will certainly reflect structure. Recognition of structurally controlled anomalies and the implications stemming from their association with fluid movement adds an important dimension to exploration strategies.

Acknowledgments

Waukaroo Bore
Strike : N19°
Dip : 82° to N109°

Acacia Vale
Strike : N38°
Dip : 74° to N128°

Sculptures / Archery Range
Strike : N46°
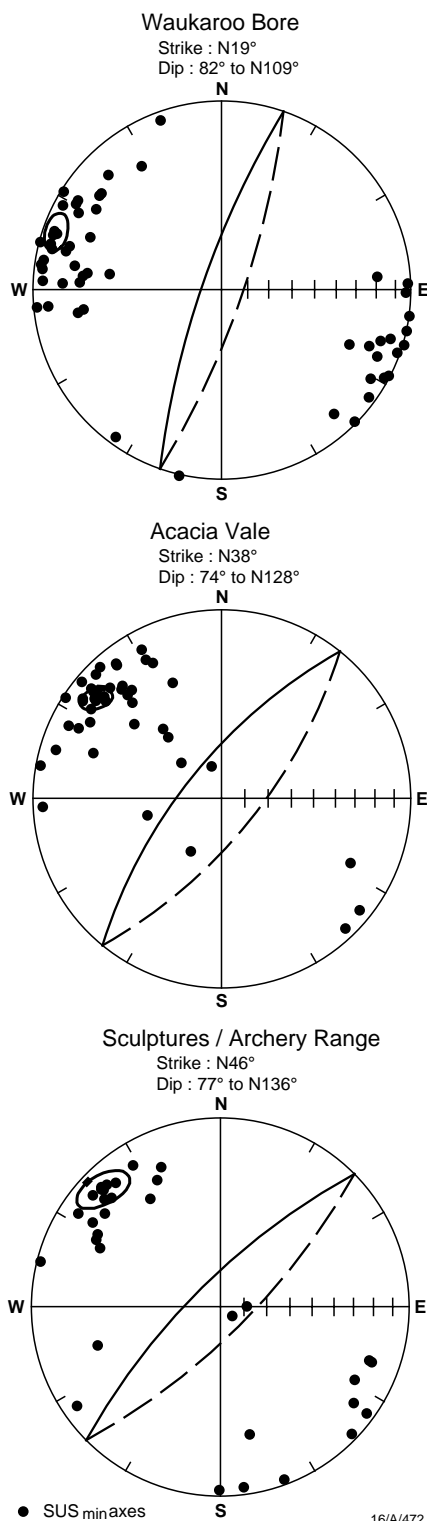Dip : 77° to N136°

● SUS $_{min}$ axes

16/A/472

Fig. 6. AMS is characterised by a susceptibility ellipsoid defined by the directions and magnitudes of the maximum (k_{max}), intermediate (k_{int}), and minimum (k_{min}) susceptibilities. This diagram shows the planes of maximum magnetic susceptibility — petrofabric planes containing the mean k_{max} and mean k_{int} axes — for the three anomalies WB, AV, and SA and mean poles (mean k_{min} axes with 95% confidence ellipses) to those planes (lower-hemisphere equal-angle projections; solid lines — traces of the planes on the upper hemisphere; dots — measurements of k_{min} axes for individual samples). Note that the planes dip steeply to ESE or SE, and veer in azimuth from ENE in the north to NE in the southern localities, showing (by comparison with Fig. 5) that the AMS is tracking the S_3 fabric.
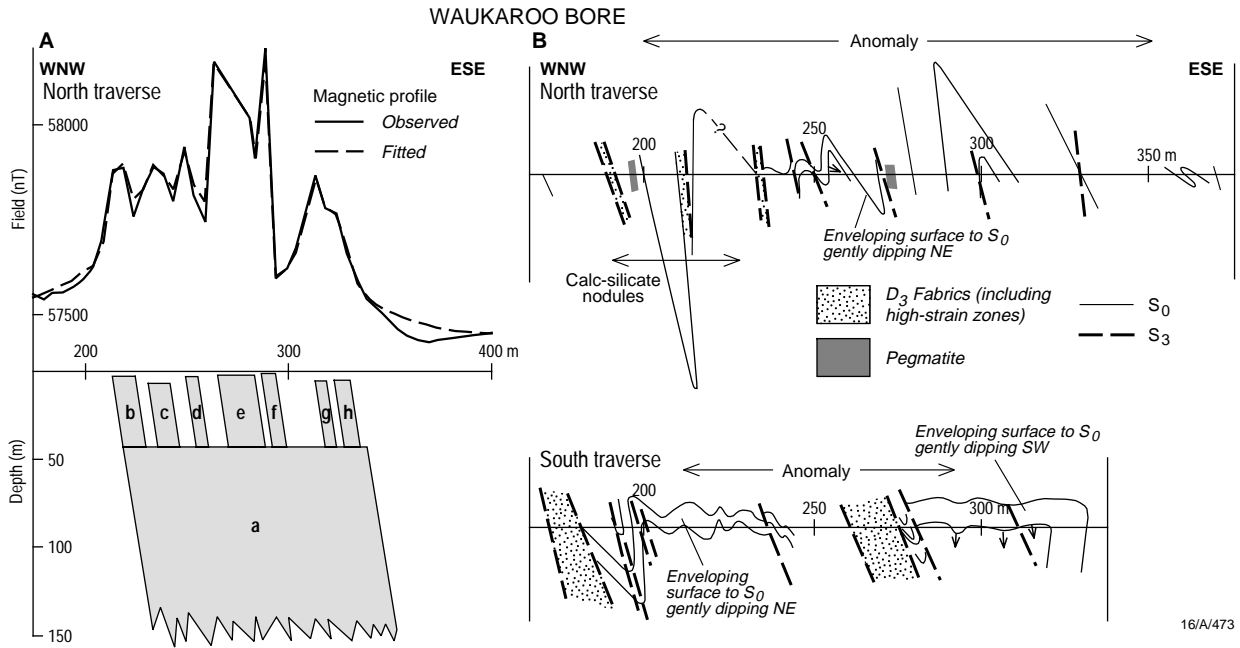
WAUKAROO BORE

Fig. 7. Waukaroo Bore anomaly showing: (A) the anomalous part of the magnetic profile for the north traverse (two traverses were made 500 m apart along the strike of the anomaly) and, using induced and remanent magnetisation, our interpreted steeply dipping source body of great depth extent and narrower near-surface bodies (a–h represent bodies with the following susceptibilities in 10^{-5} SI — a, e, f, g: 4500; b, d: 1800; c: 3000; h: 2500 — lower values of susceptibility in the narrow near-surface bodies most likely reflect weathering); (B) the structural cross-sections for relevant parts of both the north and south traverses illustrating that the enveloping surface to bedding (S_0) is not steeply dipping but is gently dipping either to the NE or SW and that the S_3 fabric dips steeply to the ESE like our modelled source geometry. We have a clear case of structural rather than stratigraphic control of this anomaly.
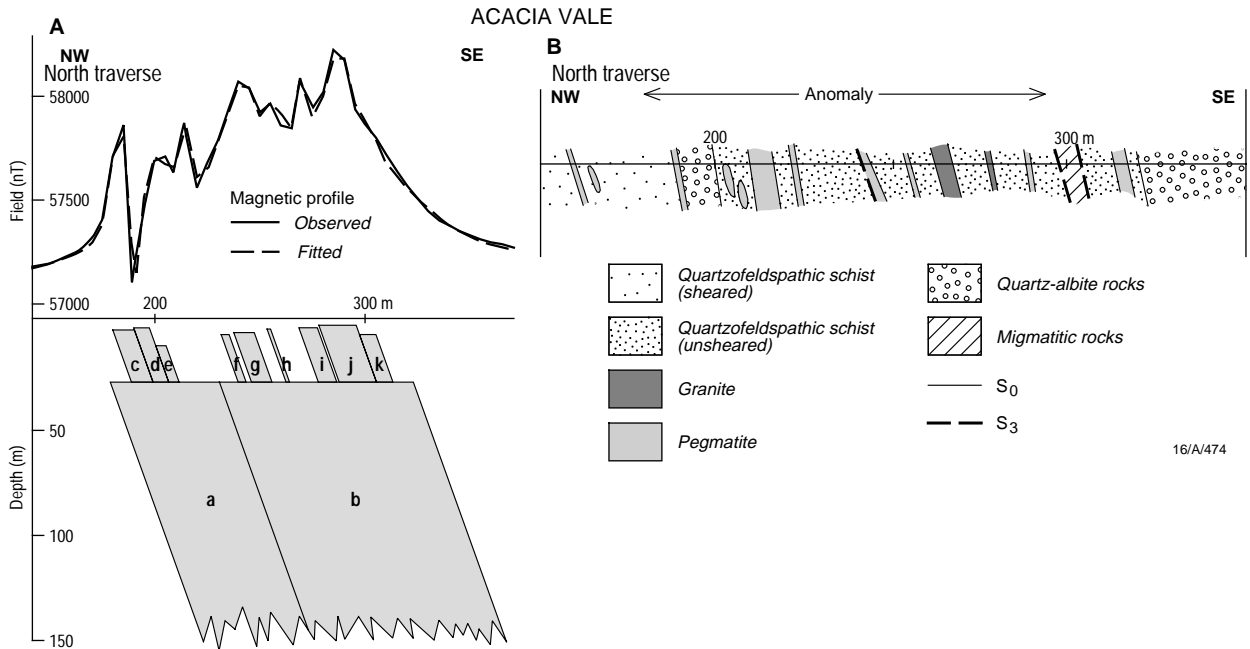
ACACIA VALE

Fig. 8. Acacia Vale anomaly showing: (A) as in Fig. 8a, our interpreted source geometry for the north traverse magnetic profile (susceptibilities in 10^{-5} SI for a–k — a,k: 2000; b: 5000; c: 1100; d: 2500; e: 4800; f,i: 1200; g: 1700; h: 1900; j: 3200; the lower susceptibility for part of the deep body, a, is consistent with geological evidence for magnetite depletion in this zone owing to bleeding of magnetite into the reactivated fabric of the adjacent retrograde shear zone); (B) structural cross-section for the traverse illustrating that bedding (S_0) and S_3 have similar steep dips, so that the case for structural control can be challenged on the basis that S_3 could have inherited a pre-existing magnetite-rich S_0 fabric (stratigraphic control).